

Dynamical vertex mass generation and chiral symmetry breaking on the light-front

Matthias Burkardt
 Department of Physics
 New Mexico State University
 Las Cruces, NM 88003-0001
 U.S.A.

Naively, helicity flip amplitudes for fermions seem to vanish in the chiral limit of light-front QCD, which would make it nearly impossible to generate a small pion mass in this framework. Using a simple model, it is illustrated how a large helicity flip amplitude is generated dynamically by summing over an infinite number of Fock space components. While the kinetic mass is basically generated by a zero-mode induced counter-term, the vertex mass is generated dynamically by infinitesimally small, but nonzero, momenta. Implications for the renormalization of light-front Hamiltonians for fermions are discussed.

I. INTRODUCTION

Deep inelastic lepton-hadron scattering has played a fundamental role in the investigation of hadron structure. For example, the discovery of Bjorken scaling confirmed the existence of point-like charged objects inside the nucleon (quarks). Besides such fundamental discoveries, deep inelastic scattering (DIS) revealed surprising and interesting details about the structure of nucleons and nuclei, such as the nuclear EMC effect, the spin crisis in polarized DIS experiments and the isospin asymmetry of the nucleon's Dirac sea.

Perturbative QCD evolution has been successfully applied to correlate large amounts of experimental data. However, progress in understanding non-perturbative features of the parton distributions in these experiments has been slow. In fact, the theoretical understanding of the surprising results listed above is mostly limited to *ad hoc* models with little connection to the underlying quark and gluon degrees of freedom.

Part of the difficulty in describing parton distributions nonperturbatively derives from the fact that parton distributions measured in DIS are dominated by correlations along the light-cone ($x^2 = 0$). For example, this makes calculations of parton distributions on a Euclidean lattice, where all distances are space-like, very difficult. Furthermore, in an equal time quantization scheme, deep inelastic structure functions are described by real time response functions which are not only very difficult to interpret but also to calculate.

Light-front (LF) quantization provides the most physical approach towards calculating the quark-gluon structure of hadrons measured in deep-inelastic lepton-nucleon scattering experiments [1–3]. Furthermore, LF quantization seems to be a promising tool to describe the im-

mense wealth of experimental information about structure functions since correlations along the light-cone become “static” observables in this approach [i.e. equal $x^+ \equiv (x^0 + x^3)/\sqrt{2}$ observables]. This implies that parton distribution functions are easy to evaluate from the LF wavefunctions and are easily interpreted as LF momentum densities. Similar simplifications apply to many other high-energy scattering observables, including non-forward parton distributions measurable in deeply virtual Compton scattering experiments [4].

Further advantages of the LF formalism derive from the simplified vacuum structure (nontrivial vacuum effects can only appear in zero-mode degrees of freedom) which provides a physical basis for the description of hadrons that stays close to intuition: fields are quantized at equal LF-time $x^+ = (x^0 + x^3)/\sqrt{2}$. As a result, the longitudinal momentum p^+ for all quanta is both a kinematical operator (no interactions) and strictly positive (as long as zero-modes, i.e. modes with p^+ strictly zero, are not explicitly included as dynamical degrees of freedom). Since the Fock-vacuum has vanishing p^+ momentum, this implies that interactions cannot mix states that contain particle hole excitations on top of the Fock vacuum with the Fock vacuum itself, and hence the full vacuum is the Fock vacuum. The resulting apparent contradiction between nontrivial vacua in a conventional formulation of quantum field theory and trivial vacua on the LF is resolved upon realizing that one should not merely omit zero-mode degrees of freedom from LF Hamiltonians but rather integrate them out which results in the concept of effective LF-Hamiltonians [1,3,5]. In such an approach the vacuum structure is shifted from the states to the operators (e.g. the Hamiltonian) and one can (at least in principle) account for nontrivial vacuum structure in the renormalization procedure.

Constructing effective LF Hamiltonians is in general a nontrivial task. For a variety of model field theories, this task has been successfully accomplished (examples can be found in Refs. [1,3,6–8]) and as far as theories with fermions is concerned, the following general features emerge:

In the LF-formulation, only half of the spinor components are dynamical degrees of freedom in the sense that their equation of motion involves a time derivative. Upon introducing $\psi_{(\pm)} = \gamma^\pm \gamma^\mp \psi / 2$, one finds for example in QCD that $\psi_{(-)}$ satisfies a constraint equation [1]

$$i\partial_- \psi_{(-)} = \left[\vec{\alpha}_\perp \cdot \left(i\vec{\partial}_\perp + g\vec{A}_\perp \right) + \gamma^0 m_F \right] \psi_{(+)} \quad (1.1)$$

and $\psi_{(-)}$ is usually eliminated (using this constraint equation) from the Lagrangian before quantizing the theory. Thus the Hamiltonian contains both a term quadratic in the fermion mass (the kinetic energy term for the fermions) and one term which is linear in the fermion mass (one gluon vertex with helicity flip).

It has been known for a long time that integrating out zero-mode degrees of freedom results in a nontrivial renormalization of the quadratic (kinetic!) mass term [8,9] but the linear (helicity flip vertex!) mass term in the Hamiltonian is unaffected by strict zero modes and the “vertex mass” must be identified with the current quark mass which vanishes in the chiral limit [1,6,10].

It is very easy to see how a constituent quark picture can emerge in such an approach. However, it always seemed mysterious how one can obtain a massless π meson in such a picture without having at the same time a massless ρ : when the helicity flip term for quarks is omitted, π and ρ become partners in a degenerate multiplet [10]. The key observation to resolve this problem is that one needs to find a mechanism which dynamically generates a large helicity flip amplitude. At first this seems impossible since every LF-time ordered diagram (any order in the coupling!) which flips the helicity of the fermion contains at least one power of the vertex mass (which vanishes in the chiral limit). In this paper, we will consider a toy model in which we explicitly demonstrate that summing over all orders in (Hamiltonian) perturbation theory yields a large helicity flip amplitude even though every single term in the perturbation series vanishes in the chiral limit.

II. A MODEL WITH DYNAMICAL CHIRAL SYMMETRY BREAKING

The above argument does not rule out the possibility that summing over an infinite class of time-ordered diagrams (including an infinite number of Fock space components) can lead to divergences which can compensate for the suppression of individual diagrams. A simple model to illustrate this idea is a fermion field with (fundamental) “color” degrees of freedom coupled to the transverse components of a massive vector field (adjoint representation)

$$\mathcal{L} = \bar{\psi} \left(i\cancel{\partial} - m - g\sqrt{\frac{\pi}{N_C}}\vec{\gamma}_\perp\vec{A}_\perp \right) \psi - \frac{1}{2}\text{tr}\left(\vec{A}_\perp\Box\vec{A}_\perp + \lambda^2\vec{A}_\perp^2\right) \quad (2.1)$$

We will take the limit $N_C \rightarrow \infty$, where the planar approximation becomes exact. The factor of $\sqrt{\frac{\pi}{N_C}}$ has been included in the coupling for later convenience. It should be emphasized that even though the interactions in Eq. (2.1) resemble QCD to some extent, we regard Eq. (2.1) as neither an approximation to QCD nor a phenomenological model for hadrons. Instead we take Eq. (2.1) as

a toy model with interactions that also appear in QCD, and the motivation to study this model is to shed some light on the mechanism for chiral symmetry breaking in the LF framework in general.

The reason for choosing the model in this particular way is as follows: using a model with an infinite number of “colors” (and no self-interaction for the boson field) renders the model solvable since the ladder-rainbow approximation becomes exact. A vector coupling of the bosons to the fermions is chirally invariant, and restricting the interactions to the transverse components was done to facilitate comparisons between ET and LF solutions to the model.

This model has been introduced and studied in Ref. [6], where it has been shown to exhibit dynamical chiral symmetry breaking (D χ SB) by studying the Euclidean Dyson-Schwinger (DS) equations for the model. Furthermore, it was shown that, for example, when a transverse momentum cutoff is used both in the ET as well as the LF formulation then both formulations are equivalent to all orders in perturbation theory provided the current mass in the ET framework is identified with the vertex mass¹ and if an appropriate counter-term (which arises from integrating out zero-mode degrees of freedom) is added to the kinetic mass term². This result clearly shows that while integrating out zero-modes causes kinetic mass generation for the fermions, it does not modify the only spin dependent term in the LF Hamiltonian (the helicity flip vertex which has a coupling proportional to the current mass). Thus fermion spin degrees of freedom seem to decouple in the chiral limit. If spin would really decouple, then the π and ρ (any helicity) should become degenerate, i.e. either both the π and the ρ should be massless or both be massive. Both possibilities would contradict the ET calculation (which has been shown to be equivalent to the LF calculation to all orders) where one can prove Goldstone’s theorem explicitly.

The resolution to this apparent paradox is that the above argument about the supposed degeneracy of π and ρ contains a flaw: while helicity flip amplitudes for *bare* fermions are indeed proportional to the current mass, it is conceivable that “dressing the fermions”, i.e. summing over an infinite number of Fock space components, leads to divergences in the chiral limit, which cancel the vanishing of the helicity flip coupling and lead to finite helicity flip for physical fermions and hence a nonzero π - ρ splitting.

In this paper, we will investigate a particular approximation to the above model [Eq. (2.1)], and we will

¹This is the mass term which appears in the helicity flip coupling in the LF Hamiltonian. Below we will define all couplings in the Hamiltonian in an approximation to the model.

²This is the quadratic mass term which appears in the fermion kinetic energy term in the LF Hamiltonian.

demonstrate explicitly that, even with a helicity flip vertex proportional to the current mass, finite helicity flip amplitudes are obtained for physical states in the chiral limit and that it is crucial to sum over an infinite number of Fock components in order to obtain this result.

III. DYNAMICAL VERTEX MASS GENERATION

Even though the rainbow approximation is solvable in any number of dimensions, we will restrict ourselves to a dimensionally reduced version of the above model (2.1), i.e. we will assume that the fields depend on longitudinal coordinates only, but still have the full four component γ -matrix structure.

Canonical quantization thus yields for the LF-Hamiltonian of the model

$$\begin{aligned}
H = & \sum_h \int_0^\infty dk \left[\frac{m_{kin}^2}{2k} b_{k,h,\alpha}^\dagger b_{k,h,\alpha} + \frac{\lambda^2}{2k} a_{k,h,\alpha,\beta}^\dagger a_{k,h,\alpha,\beta} \right] \\
& + \frac{g}{2\sqrt{N_C}} \sum_h \int_0^\infty dpdq \frac{dk}{\sqrt{k}} b_{p,h,\alpha}^\dagger \left(\frac{m_V}{p} - \frac{m_V}{q} \right) \times \\
& \left[\delta(p-q-k) a_{k,h,\alpha,\beta} - \delta(p+k-q) a_{k,-h,\alpha,\beta}^\dagger \right] b_{q,-h,\beta} \\
& + \frac{g^2}{2N_C} \sum_h \int_0^\infty dpdq \frac{dkdr}{\sqrt{kr}} b_{p,h,\alpha}^\dagger \times \\
& \left[\frac{\delta(p+k-q-r)}{p+k} a_{k,-h,\alpha,\beta}^\dagger a_{r,-h,\beta,\gamma} \right. \\
& \quad + \frac{\delta(p+k+r-q)}{p+k} a_{k,-h,\alpha,\beta}^\dagger a_{r,h,\beta,\gamma}^\dagger \\
& \quad \left. + \frac{\delta(p-k-r-q)}{r+q} a_{k,h,\alpha,\beta} a_{r,-h,\beta,\gamma} \right] b_{q,h,\gamma}
\end{aligned} \tag{3.1}$$

where h labels the helicity of the fermion/boson and Greek indices represent color (note that one can also drop color indices completely as long as one keeps track of the color ordering in the Fock space). Because of the large N_C limit and because we are studying the vertex of a fermion in this paper, quark pair creation can be neglected and all terms involving antiquarks are not shown in Eq. (3.1).

Helicity is conserved at each vertex in this dimensionally reduced model, which implies that fermion helicity flips in each one boson emission or absorption process and the helicity of the emitted boson will have the same sign as the helicity of the fermion before the emission. In the large N_C limit, bosons dressing a fermion must always be absorbed in reverse order to the order in which they have been emitted. Thus it makes sense to label the bosons in a given Fock state in the order in which they have been produced. This is the most convenient way to represent a state in this model. In particular, using the abovementioned helicity selection rules for this model, one can easily convince oneself that for any state which mixes with a bare fermion, the sign of the helicity for the

bosons alternates as one moves along the state (which is ordered using the rule described above). Thus it is not necessary to keep track of helicity degrees of freedom explicitly, and we will completely omit helicity labels from now on.³

In the canonical Hamiltonian there is only one fermion mass $m_{kin} = m_V = m$, but in general, when zero-mode degrees of freedom have been integrated out, one has to distinguish between m_{kin} and m_V .⁴

The only interaction term in Eq. (3.1) which flips the helicity of the quarks is the 3-point coupling, which is proportional to m_V .⁵

In the following, we will study corrections to the vertex of the A_\perp -field in Hamiltonian perturbation theory. This analysis is greatly simplified due to the large N_C limit for the following two reasons: First of all, the only ‘‘vertex corrections’’ are actually given by diagrams that resemble a self energy correction to the external legs which are connected to the ‘‘external’’ vertex by an instantaneous interaction. Secondly, the rainbow approximation for self-energies becomes exact.

In order to organize the perturbative expansion, it is useful to introduce some notation and graphical symbols representing the notation in time-ordered diagrams. First we introduce the fermion Green’s function $G(p, E)$. For a free theory $G(p, E) = 1/(E - \frac{m^2}{2p} + i\varepsilon)$, while for an interacting theory

$$G(p, E) = \sum_n \frac{p_n(1)}{E - E_n + i\varepsilon}, \tag{3.2}$$

where the sum is over eigenstates of the Hamiltonian with momentum p and energy eigenvalue E_n and where $p_n(1)$ denotes the probability to find the n -th state in the lowest Fock component. In diagrams, all propagating (i.e. non-instantaneous) fermion lines are implicitly assumed to represent the full Green’s function $G(p, E)$.

³There are two equivalent ways how one can recover the hidden helicity information for a dressed fermion: from the wave function by counting the number of ‘‘gluons’’ (an odd number means the helicity of the fermion is reversed to its helicity in the bare Fock component), or by counting the number of ‘‘gluons’’ in an intermediate state in perturbation theory.

⁴The only exception seem to be calculations where a Pauli-Villars regulator is used (see Refs. [9,11] and references therein).

⁵Note that total helicity ($h_q + 2h_g$) is conserved at each vertex, which follows from the fact that setting the x and y components of all momenta equal to zero is rotational invariant about the z axis.

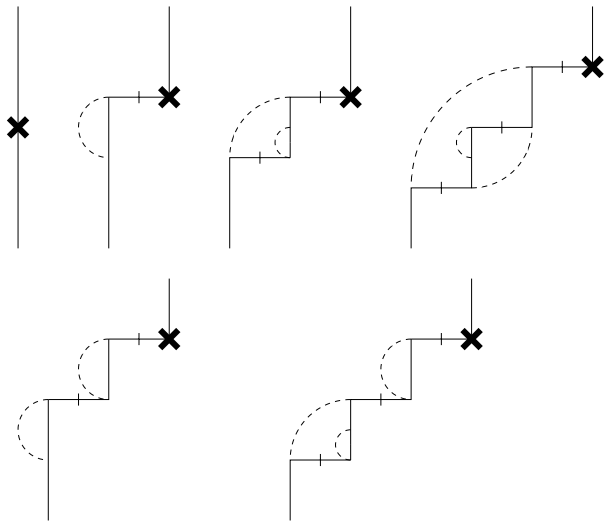


FIG. 1. Typical LF-time ordered diagrams contributing to the helicity flip amplitude (one “gluon” vertex) for a fermion in planar approximation. The external gluon vertex is depicted by a cross. The dashed lines are boson fields and the slashed lines represent LF-instantaneous interactions. Since the instantaneous interactions conserve fermion helicity, the actual helicity flip occurs at the non-instantaneous vertex inside the loop corrections. Only diagrams with corrections to the incoming fermion line are drawn, but the corrections might instead occur on the outgoing line.

Vertex corrections in the model can only occur on either the incoming or the outgoing line, but not on both at the same time.⁶ It thus makes sense to decompose the full vertex function $\Gamma(p, p', E)$ (denoted by a full blob) into the bare piece, corrections to the incoming line $\Gamma_i(p, E)$ (denoted by a full semicircle on the incoming line and connected via an instantaneous interaction to the external vertex) as well as corrections to the outgoing line $\Gamma_o(p', E)$ (denoted by a full semicircle on the outgoing line and connected via an instantaneous interaction to the external vertex).⁷

$$\Gamma(p, p', E, E') = \left(\frac{m_V}{2p} - \frac{m_V}{2p'} \right) + \Gamma_o(p', E') + \Gamma_i(p, E), \quad (3.3)$$

⁶With the exception of theories that contain couplings to “bad currents” (such as a coupling involving $\bar{\psi}\gamma^-\psi$) there cannot be two instantaneous interactions couple to the same vertex. In the above example, this can be seen explicitly by using γ^+/p^+ for the instantaneous propagator and by using the γ -algebra $\gamma^+\gamma_\perp\gamma^+ = 0$.

⁷Actually, there is a very simple relation between vertex corrections on the incoming and outgoing lines, $\Gamma_i(p, E) = -\Gamma_o(p, E)$, but we found it useful to distinguish them in order to better elucidate the details of the recursive relations.

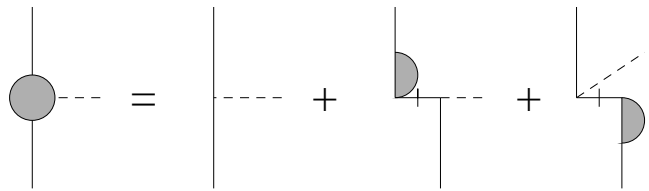


FIG. 2. Decomposition of the full vertex into the bare vertex, corrections attached to the outgoing line and corrections to the incoming line.

where E and E' are related by energy conservation. They satisfy the integral relations

$$\Gamma_i(p, E) = \frac{g^2}{p} \int_0^p \frac{dk}{2k} G(p-k, E - \frac{\lambda^2}{2k}) \times \left[\frac{m_V}{2p} + \Gamma_i(p, E) - \frac{m_V}{2(p-k)} + \Gamma_o(p-k, E - \frac{\lambda^2}{2k}) \right] \quad (3.4)$$

$$\Gamma_o(p', E') = \frac{g^2}{2p'} \int_0^{p'} \frac{dk}{2k} G(p'-k, E' - \frac{\lambda^2}{2k}) \times \left[\frac{m_V}{2(p'-k)} + \Gamma_i(p'-k, E' - \frac{\lambda^2}{2k}) - \frac{m_V}{2p'} + \Gamma_o(p', E') \right], \quad (3.5)$$

which have been illustrated in Fig. 3

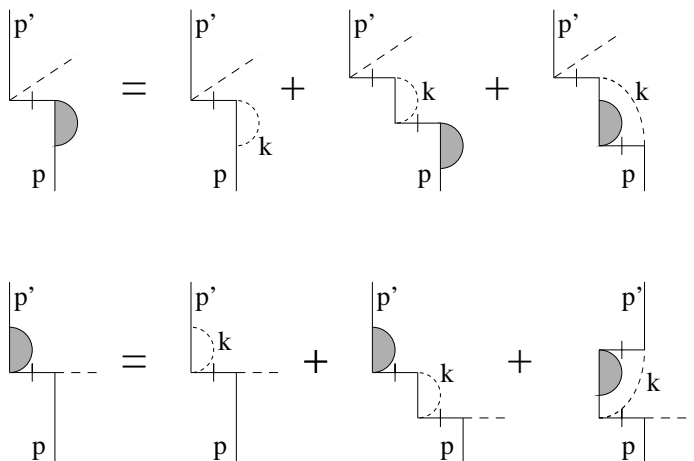


FIG. 3. Recursive relation between loop corrections for the dressed vertex.

Given the Green’s function, one can thus calculate Γ nonperturbatively, by solving Eqs. (3.3-3.5) self-consistently (e.g. by iteration).

In order to calculate the Green’s function $G(p, E)$, it is useful to divide up all self energies Σ into two main classes: those which do not involve helicity flip (except in sub-diagrams) $\Sigma^{no\ flip}$ and those where the outermost “gluon” loop does involve double helicity flip Σ^{flip} .

$$\Sigma(p, E) = \Sigma^{flip}(p, E) + \Sigma^{no\ flip}(p, E). \quad (3.6)$$

They satisfy (Fig. 4)

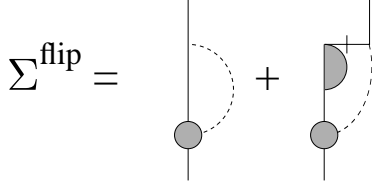


FIG. 4. Self-energy generated by two consecutive (dressed) helicity flip interactions. For the second vertex, dressing on the “outside” has to be excluded in order to avoid double counting.

$$\Sigma^{flip}(p, E) = g^2 \int_0^p \frac{dk}{k} \Gamma(p, p-k, E, E - \frac{\lambda^2}{2k}) \times \quad (3.7)$$

$$G(p-k, E - \frac{\lambda^2}{2k}) \times$$

$$\left[\frac{m_V}{2p} - \frac{m_V}{2(p-k)} + \Gamma_i(p-k, E - \frac{\lambda^2}{2k}) \right]$$

as well as (Fig. 5)

$$\Sigma^{noflip} = \frac{g^2}{2} \int_0^p \frac{dk}{(p-k)k} \frac{\Sigma^{di}(p-k, E - \frac{\lambda^2}{2k})}{1 - \Sigma^{di}(p-k, E - \frac{\lambda^2}{2k})} \quad (3.8)$$

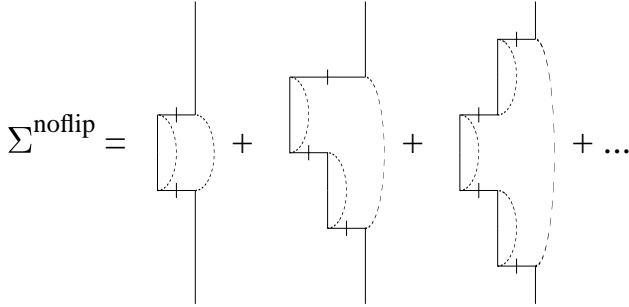


FIG. 5. Self energy diagrams without helicity flip.

where the “double instantaneous” self energy Σ^{di} is given by

$$\Sigma^{di}(p, E) = \frac{g^2}{2p} \int_0^p \frac{dk}{k} G(p-k, E - \frac{\lambda^2}{2k}). \quad (3.9)$$

Finally, one can calculate the Green’s function from the self-energies using

$$G(p, E) = \frac{1}{E - \frac{m_{kin}^2}{2p} - \Sigma(p, E)}. \quad (3.10)$$

The above set of equations allows one to determine both self-energy and vertex functions in a self-consistent manner. The solution to these integral equations is completely non-perturbative and should thus contain the physics of $D\chi SB$.

IV. AN ILLUSTRATIVE EXAMPLE: $\lambda \rightarrow \infty$

In general the coupled integral equations relating vertex and self-energy need to be solved numerically. However, in this section we will illustrate the physics of these equations by considering the limiting case where the “gluon” mass is very large and thus all loop diagrams become energy independent — the Gross-Neveu limit.

For example, the Green’s function becomes that of a free particle

$$G(p, E) = \frac{1}{E - \frac{M_{phys}^2}{2p} + i\varepsilon}. \quad (4.1)$$

Below we will show this result explicitly and we will also determine M_{phys} self-consistently. For $\lambda \rightarrow \infty$, not only self energies, but also the “vertex-corrections” Γ become energy independent and one can thus parameterize them in the form

$$\Gamma_i(p, E) = -\Gamma_o(p, E) = \frac{\Delta M_V}{2p}. \quad (4.2)$$

From Eqs. (3.4) one finds for example

$$\Gamma_i(p, E) = \frac{g^2}{2p} \int_0^1 \frac{dx}{1-x} \frac{M_V}{\frac{M_{phys}^2}{1-x} + \frac{\lambda^2}{x} - 2pE}$$

$$\xrightarrow{\lambda^2 \rightarrow \infty} \frac{M_V}{2p} \frac{g^2}{\lambda^2} \ln \frac{\lambda^2}{M_{phys}^2} \quad (4.3)$$

where $M_V \equiv m_V + \Delta M_V$, and where we take the limit $\lambda^2 \rightarrow \infty$ in such a way that $\frac{g^2}{\lambda^2} \ln(\lambda^2/M_{phys}^2)$ remains fixed in order to obtain a nontrivial limit. Thus, combining Eq. (4.2) with Eq. (4.3), one finally obtains

$$M_V = m_V + \frac{M_V g^2}{\lambda^2} \ln \frac{\lambda^2}{M_{phys}^2}, \quad (4.4)$$

i.e.

$$M_V = \frac{m_V}{1 - \frac{g^2}{\lambda^2} \ln \frac{\lambda^2}{M_{phys}^2}}. \quad (4.5)$$

This result can now be used to evaluate the self-energy and hence the physical mass M_{phys} . In order to avoid having to deal with any zero mode degrees of freedom, we implicitly use a Pauli-Villars (PV) regulator, where the kinetic mass counter-term induced by zero-modes is known to vanish (see for example Refs. [9,11]).

First of all one finds that the “double-instantaneous” self-energy Σ^{di} (3.9) vanishes for $\lambda^2 \rightarrow \infty$, since it does not contain the $\ln \lambda^2$.

$$\Sigma^{di} \xrightarrow{\lambda^2 \rightarrow \infty} \frac{g^2}{2p\lambda^2} \propto \frac{1}{\ln \frac{\lambda^2}{M_{phys}^2}} \xrightarrow{\lambda^2 \rightarrow \infty} 0 \quad (4.6)$$

and thus Σ^{noflip} (3.8) can be neglected.

For Σ^{flip} , which is the only divergent self-energy in this model, a PV regulator is used at intermediate steps.⁸ After a few trivial algebraic steps [9,11], one eventually finds

$$\begin{aligned}\Sigma^{flip} &= \frac{g^2}{2p} \int_0^1 \frac{dx}{x} \frac{\left(M_V - \frac{M_V}{1-x}\right) \left(m_V - \frac{M_V}{1-x}\right)}{2pE - \frac{M_{phys}^2}{1-x} - \frac{\lambda^2}{x}} \\ &\xrightarrow{PV} -\frac{g^2}{2p} \int_0^1 \frac{dx}{x} \frac{\left[m_V M_V \frac{x}{1-x} + \frac{M_V^2}{1-x} + 2pE\right]}{2pE - \frac{M_{phys}^2}{1-x} - \frac{\lambda^2}{x}} \\ &\xrightarrow{\lambda^2 \rightarrow \infty} M_V (m_V + M_V) \frac{g^2}{2p\lambda^2} \ln \frac{\lambda^2}{M_{phys}^2},\end{aligned}\quad (4.7)$$

which is energy independent and thus confirms the original ansatz for $G(p, E)$ Eq. (4.1). Using Eqs. (3.10) and (4.1) one thus finds

$$M_{phys}^2 = m_V^2 + M_V (m_V + M_V) \frac{g^2}{\lambda^2} \ln \frac{\lambda^2}{M_{phys}^2}. \quad (4.8)$$

Note that we made use here of the fact that the kinetic mass m_{kin} in the Hamiltonian and the bare vertex mass m_V are identical when a PV regulator is employed [9,11].

In order to disentangle the relation between bare vertex mass m_v , dynamical vertex mass M_V and the physical mass M_{phys} , we use Eq. (4.4) to eliminate the logarithm in Eq. (4.8), yielding

$$M_{phys}^2 = m_V^2 + M_V (m_V + M_V) \frac{(M_V - m_V)}{M_V} = M_V^2, \quad (4.9)$$

i.e. in this simple example, the consistent solution of the coupled system of equations for the vertex function and the self-energy yields a physical mass which is identical to the dynamical vertex mass. Note that this equality of M_{phys} (defined through the lowest eigenvalue of the invariant mass operator) and M_V (defined through the helicity flip amplitude) is a nontrivial result. In more general models, one would still expect that there are some connections between M_{phys} (or a constituent mass) and M_V but they do not necessarily have to be numerically equal.

Furthermore, if we use this identity between M_{phys} and M_V in Eq. (4.4) [or in Eq. (4.8)], one finds that

$$M_V = m_V + M_V \frac{g^2}{\lambda^2} \ln \frac{\lambda^2}{M_V^2} \quad (4.10)$$

which is not only identical to the covariant ‘‘gap equation’’ for this model, but which also admits a nonzero solution for M_V in the chiral limit ($m_V \rightarrow 0$)

$$M_{phys} = M_V = \lambda e^{-\frac{\lambda^2}{2g^2}}, \quad (4.11)$$

i.e. a nonzero vertex mass has been generated dynamically. Obviously, Eq. (4.11) is non-perturbative in the coupling constant, but this should not be too surprising since, even though we used diagrammatic techniques, what we have done is in fact solved a bound state problem and bound states are always non-perturbative.

From Eq. (4.5) one would naively expect that the physical vertex mass M_V vanishes in the chiral limit, i.e. when the bare vertex mass m_V vanishes. However, a glance at Eq. (4.11) reveals that the denominator of Eq. (4.5) also vanishes in the chiral limit. When one performs a perturbation expansion of the physical helicity flip amplitude in the coupling g , one finds that every single diagram vanishes in the chiral limit, since every helicity flip diagram contains at least one helicity flip interaction which is proportional to m_V . However, upon summing over an infinite number of diagrams, one obtains a divergent geometric series which compensates for the vanishing of m_V . In fact, substituting M_{phys} for M_V in Eq. (4.8), one finds that

$$1 - \frac{g^2}{\lambda^2} \ln \frac{\lambda^2}{M_{phys}^2} = \frac{m_V}{M_{phys}} \quad (4.12)$$

which explicitly shows the vanishing of the denominator in Eq. (4.5) for $m_V \rightarrow 0$.

From the practitioner’s point of view, it is very important to know how a dynamically generated vertex mass would in principle emerge in a Fock space expansion. In order to elucidate this point, let us suppose that we know M_{phys} , but not M_V and let us attempt to determine M_V perturbatively. For this purpose, let us consider a helicity flip process and focus on all those diagrams which are linear in the vertex mass, i.e. contain only one helicity flip vertex. Since we suppose that we know the physical mass, it makes sense to redefine the kinetic mass as the physical mass, but then one should no longer take into account diagrams with self-mass sub-diagrams⁹ since this would amount to double counting. Without self-mass sub-diagrams and in the planar approximation considered here, this leaves only a very simple class of diagrams which are linear in the vertex mass. In the following, we will study this class in detail and sum it up to all orders in perturbation theory.

First of all, since we work in a dimensionally reduced model, boson-fermion vertices are linear in the vertex mass, unless they are instantaneous vertices, i.e. the limitation to terms linear in the vertex mass means that all but one vertex in a given time ordered diagram must be instantaneous. This means that, to leading order in the

⁸An alternative, which we will not pursue in this paper, would be to include a separate kinetic mass counter-term.

⁹I.e. sub-diagrams with only two external fermion lines, which are both on mass shell.

vertex mass, a general higher order diagram for a helicity flip vertex is obtained by attaching an instantaneous interaction to the external vertex and then another one to the boson line emanating from the first instantaneous vertex and so on until the last boson line ends up in the actual helicity flip vertex. Typical diagrams are depicted in Fig. 2¹⁰

Let us first look at the “bare rainbow” diagrams¹¹ in the top row of Fig. 2.

We will restrict ourselves to vertex corrections in the incoming state. Furthermore, in order to simplify the notation, we absorb a trivial kinematic factor into the definition of the helicity-flip amplitude by introducing

$$T_{flip} \equiv 2p\Gamma_i. \quad (4.13)$$

The first diagram in Fig. 2 is just the bare vertex. The second diagram yields (Fig.6a)

$$T_{flip}^{2a} = m_V g^2 I_1, \quad (4.14)$$

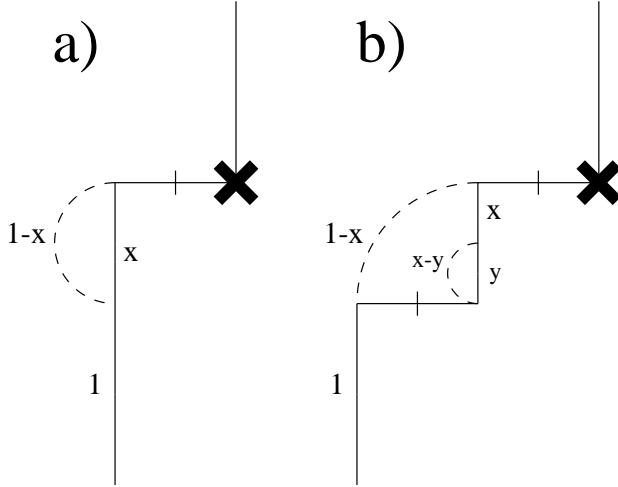


FIG. 6. Lowest order bare rainbow diagrams.

where

$$I_1 = \int_0^1 \frac{dx}{(1-x)} \frac{\frac{1}{x} - 1}{2pE - \frac{M_{phys}^2}{x} - \frac{\lambda^2}{1-x}} \xrightarrow{\lambda \rightarrow \infty} \frac{1}{\lambda^2} \ln \frac{\lambda^2}{M_{phys}^2}. \quad (4.15)$$

¹⁰Of course, in addition to the diagrams in Fig. 2, there are corrections to the helicity flip amplitude on the other side of the external vertex, but up to kinematical factors, these are identical to the ones depicted in Fig. 2.

¹¹We call these diagrams bare rainbow diagrams, since they really have the topology of a rainbow, as distinguished from iterated or nested rainbows.

The fourth order bare rainbow is a little more complicated, yielding (up to the same overall factors as Eq. (4.14) (Fig. 6b)

$$T_{flip}^{2b} = g^4 m_V \int_0^1 \frac{dx/(1-x)}{2pE - \frac{M_{phys}^2}{x} - \frac{\lambda^2}{1-x}} \times \int_0^x \frac{dy/(x-y) \left(\frac{1}{y} - \frac{1}{x}\right)}{2pE - \frac{M_{phys}^2}{y} - \frac{\lambda^2}{x-y} - \frac{\lambda^2}{1-x}}. \quad (4.16)$$

The x integral in Eq. (4.16) is dominated by small values of x as $\lambda \rightarrow \infty$. This allows us to simplify the y integral ($z = y/x$)

$$\begin{aligned} & \int_0^x \frac{dy}{x-y} \frac{\left(\frac{1}{y} - \frac{1}{x}\right)}{2pE - \frac{M_{phys}^2}{y} - \frac{\lambda^2}{x-y} - \frac{\lambda^2}{1-x}} \\ &= \int_0^1 \frac{dz}{1-z} \frac{\left(\frac{1}{z} - 1\right)}{x \left(2pE - \frac{\lambda^2}{1-x}\right) - \frac{M_{phys}^2}{z} - \frac{\lambda^2}{1-z}} \\ &\xrightarrow{x \rightarrow 0} - \int_0^1 \frac{dz}{1-z} \frac{\left(\frac{1}{z} - 1\right)}{\frac{M_{phys}^2}{z} + \frac{\lambda^2}{1-z}} \xrightarrow{\lambda \rightarrow \infty} -I_1, \end{aligned} \quad (4.17)$$

i.e.

$$T_{flip}^{2b} = m_V (g^2 I_1)^2. \quad (4.18)$$

It turns out that the bare rainbow diagrams form a geometric series, yielding (together with the bare vertex)

$$T_{flip}^{bare\ rainbow} = m_V \frac{1}{1 - g^2 I_1} = m_V \frac{1}{1 - \frac{g^2}{\lambda^2} \ln \frac{\lambda^2}{M_{phys}^2}}. \quad (4.19)$$

Besides the bare rainbow diagrams one also needs to consider the nested rainbow diagrams (bottom row of Fig. 2), where the the direction of the chain of instantaneous interactions does not always alternate along the fermion line. These can be obtained from the bare rainbow diagrams by replacing each instantaneous interaction by a chain of instantaneous interactions (Fig. 7)

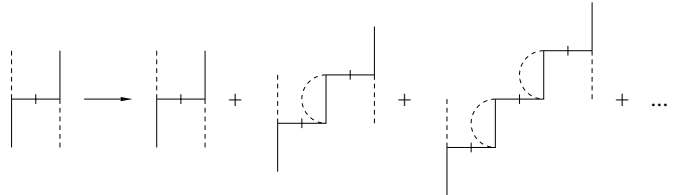


FIG. 7. Chain of instantaneous interactions leading to a geometric series.

leading again to a geometric series as $\lambda \rightarrow \infty$ ¹², which can be incorporated into above result by making the replacement

$$g^2 \longrightarrow \frac{g^2}{1 - g^2 I_2}, \quad (4.20)$$

where

$$I_2 = \int_0^1 \frac{dx}{(1-x)} \frac{1}{p^2 - \frac{M^2}{x} - \frac{\lambda^2}{1-x}} \xrightarrow{\lambda \rightarrow \infty} \frac{1}{\lambda^2} \quad (4.21)$$

in each instantaneous interaction. Together with Eq. (4.19), this yields for the sum of all planar helicity flip diagrams in leading order in the vertex mass

$$T_{flip}^{rainbow} = \frac{m_V}{1 - g^2 \frac{I_1}{1 - g^2 I_2}}. \quad (4.22)$$

However, since

$$I_2/I_1 \sim 1/\ln \lambda^2 \xrightarrow{\lambda \rightarrow \infty} 0 \quad (4.23)$$

, one can neglect I_2 in Eq. (4.22), yielding

$$T_{flip}^{rainbow} \xrightarrow{\lambda \rightarrow \infty} \frac{m_V}{1 - \frac{g^2}{\lambda^2} \ln \frac{\lambda^2}{M^2}}, \quad (4.24)$$

i.e. just the bare result above (4.19).

From our calculation above (4.12), we know already that the perturbation series diverges in the chiral limit. Eq. (4.23) tells us that the divergence arises from summing over all ‘‘bare rainbow’’ diagrams (Fig. 6).

The crucial point is that the denominator of Eq. (4.24) becomes small in the chiral limit, as one can read off from Eq. (4.12). In other words, even though each individual diagram in Fig. (2) vanishes in the chiral limit $\propto m$, summing over an infinite number of diagrams yields $T_{flip} \propto M$, which remains finite as $m \rightarrow 0$.

Several interesting observations can be made from this example:

- While zero-modes contribute significantly to the kinetic mass of fermions, there is no such zero-mode contribution to the vertex mass. However, the vertex mass gets renormalized by (infinitesimally) small x contributions since one has to sum over an infinite number of Fock space components in order to obtain a finite helicity flip amplitude in the chiral limit.
- In realistic non-perturbative calculations of hadron spectra, where one cannot include an infinite number of Fock space components, it will at some level be necessary to absorb the higher order corrections into an effective vertex mass M .

- The leading diagrams (top row in Fig. 2) have a relatively simple structure: higher order diagrams can be successively built by replacing the bare helicity flip vertex inside a given diagram with the second order dressed helicity flip vertex. This observation may be useful for a renormalization group study of the helicity flip interactions, since a large amplitude is obtained only through an infinite chain of steps from finite x down to vanishingly small values of x . Qualitatively, this mechanism resembles the chiral symmetry breaking mechanism suggested in Ref. [12].

V. DMVG IN A COVARIANT FRAMEWORK

Even though we have formulated the mechanism for DVMG entirely in the Hamiltonian LF framework, it is very instructive to rephrase the above results using covariant language. It should be emphasized that all results derived in this section are of course also contained in the LF-Hamiltonian result.

For the above model, the nonperturbatively obtained covariant self-energy (obtained for example by solving Dyson-Schwinger equations) can be expressed in the form

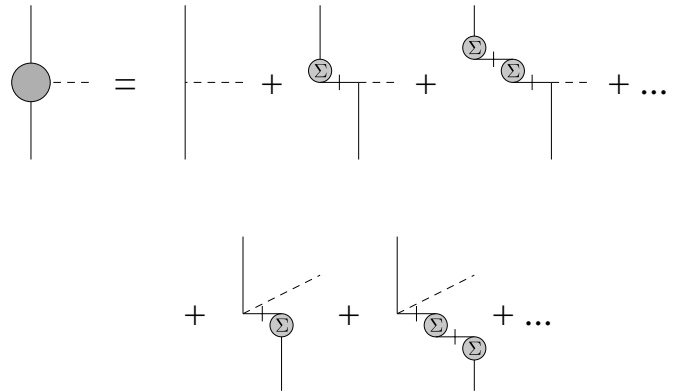
$$\Sigma = A(p^2) \not{p} + B(p^2), \quad (5.1)$$

yielding for the dressed fermion propagator

$$\begin{aligned} S &\equiv \frac{1}{\not{p} - m - \Sigma} = \frac{1}{\not{p}(1 - A(p^2)) - m - B(p^2)} \\ &= \frac{\not{p}(1 - A(p^2)) + m + B(p^2)}{p^2(1 - A(p^2))^2 - (m + B(p^2))^2}, \end{aligned} \quad (5.2)$$

where $\not{p} \equiv \gamma^+ p^- + \gamma^- p^+$ and $p^2 = 2p^+ p^-$.

Dynamical chiral symmetry breaking manifests itself as $B \neq 0$ even for vanishing current quark mass $m \rightarrow 0$. In order to compare the covariant approach with the Hamiltonian LF framework, we ask: what is the helicity flip amplitude which is in this case generated by self-energy diagrams connected to the external vertex by LF-‘‘instantaneous’’ γ^+/p^+ propagators?



¹²Only for $\lambda \rightarrow \infty$ can one neglect the energy dependence of these bubbles.

FIG. 8. Relation between the dressed LF vertex (large blob) and the covariant self-energy Σ (smaller blobs).

The resulting chain of self energy diagrams (Fig. 8) is a geometric series and one thus finds for example for the sum of all corrections attached to the incoming line

$$\begin{aligned}\Gamma_i(p^+, p^-) &= \bar{u}'\gamma_x \frac{\gamma^+}{2p^+} \Sigma u + \bar{u}'\gamma_x \frac{\gamma^+}{2p^+} \Sigma \frac{\gamma^+}{2p^+} \Sigma u \\ &\quad + \bar{u}'\gamma_x \frac{\gamma^+}{2p^+} \Sigma \frac{\gamma^+}{2p^+} \Sigma \frac{\gamma^+}{2p^+} \Sigma u + \dots \\ &= \bar{u}'\gamma_x \frac{\gamma^+}{2p^+} \Sigma u \frac{1}{1 - A(p^2)} \\ &= \frac{1}{2p^+} \frac{mA(p^2) + B(p^2)}{1 - A(p^2)}.\end{aligned}\quad (5.3)$$

Note that the spinor basis in which the LF Hamiltonian is constructed contains the current quark mass. Therefore, when taking spinor matrix elements of the covariant amplitude we must also use spinors u and \bar{u}' which also contain the current quark mass in order to be able to relate the covariant calculation to the LF-Hamiltonian calculation.

The total dressed vertex (including the bare piece as well as renormalizations on both the incoming and the outgoing line) thus reads

$$\begin{aligned}\Gamma &= \frac{1}{2p^+} \left(m + \frac{mA(p^2) + B(p^2)}{1 - A(p^2)} \right) \\ &\quad - \frac{1}{2p^{+'}} \left(m + \frac{mA(p^{2'}) + B(p^{2'})}{1 - A(p^{2'})} \right) \\ &= \frac{1}{2p^+} \left(\frac{m + B(p^2)}{1 - A(p^2)} \right) - \frac{1}{2p^{+'}} \left(\frac{m + B(p^{2'})}{1 - A(p^{2'})} \right).\end{aligned}\quad (5.4)$$

In order to understand the physics of Eq. (5.4), let us first consider the case where both the incoming and the outgoing line correspond to on-shell states, i.e. $p^2 = p^{2'} = M_{phys}^2$. Analyzing the pole structure of the fermion propagator Eq. (5.2) yields

$$M_{phys} (1 - A(M_{phys}^2)) = B(M_{phys}^2) \quad (5.5)$$

and thus

$$\Gamma = \frac{M_{phys}}{2p^+} - \frac{M_{phys}}{2p^{+'}}. \quad (p^2 = p^{2'} = M_{phys}^2). \quad (5.6)$$

The physics of Eq. (5.6) is that the physical helicity flip amplitude in this model for on-shell fermions is identical to the one for free (non-dressed) fermions with a mass equal to the physical mass of the fermions.¹³

Of course, this result changes when the fermions are far from their mass shell. In asymptotically free models, where $A(p^2), B(p^2) \rightarrow 0$ as $p^2 \rightarrow -\infty$ one recovers the current quarks

$$\Gamma \rightarrow \frac{m}{2p^+} - \frac{m}{2p^{+'}}. \quad (p^2 = p^{2'} \rightarrow -\infty). \quad (5.7)$$

Note that the dressed vertex in this model depends only on the p^2 of the initial and final state, but it does *not* depend on the momentum transfer. This feature is of course a peculiarity of the model which arises because we make a planar approximation and because the “gluons” in the model have no direct self-interaction. This feature prohibits “gluon” lines that run across the “gluon” vertex and hence the only “vertex” corrections are, from a covariant point of view, corrections to the propagators. Therefore, it is quite natural in this model that the “vertex corrections” depend only on the invariant mass of the external fermion lines.

Another interesting observation one can make is about the connection between the effective mass and condensates. Obviously, the numerator appearing in the dressed (helicity flip) vertex (5.4) is identical to the numerator of the Dirac-trace of the dressed propagator (5.2). On the other hand, the trace of the propagator appears in the expression for the Fourier transform of non-local quark condensates, which suggests that there might be a deep connection between the effective vertex mass and non-local quark condensates.¹⁴ To illustrate this point, let us consider a situation where $A(p^2) \ll 1$ and where $p^2 \gg (m + B(p^2))^2$. In this limit one obviously finds that the running vertex mass $M_V(p^2) \equiv \frac{m+B}{1-A}$ satisfies

$$M_V(p^2) = p^2 \text{tr}(S(p)). \quad (5.8)$$

Intuitively, one would also expect a relation between the running vertex mass and the local condensate. Even though we were able to establish such a relation from the integral equations determining the dressed vertex in certain limiting cases, these results did depend on model details and will thus not be displayed here.

VI. SUMMARY AND OUTLOOK

We have studied the non-perturbative enhancement of the fermion helicity flip amplitude in a simple model formulated in the LF framework. The dimensionally reduced model, consisting of fermions coupling to the transverse component of a vector field, treated in planar approximation (“large N_C ”), is of course quite different

¹³Note that in similar situations in the ET approach, it is convenient to perform a Bogoliubov transformation [14], which yields large helicity flip amplitudes due to self-energies in a more direct way than in the LF approach.

¹⁴For a recent study of non-local condensates, see for example Ref. [13].

from real QCD, and one cannot consider it an approximation to QCD or a phenomenological model for QCD. What the model has in common with QCD is that it is based on a chirally invariant Lagrangean and that the chiral symmetry is dynamically broken, leading for example to mass generation for the fermions in the limit of vanishing current quark masses. It is because of this similarity that we believe that studying its features in the LF framework may shed some light on how dynamical chiral symmetry breaking might perhaps arise in LFQCD.

In this model, we were able to show that even though every perturbative diagram for helicity flip amplitudes is proportional to at least one power of the vertex mass (=current mass), and thus vanishes in the chiral limit, the sum over all diagrams yields a result which remains finite for vanishing vertex mass. In a solvable model, which resembles the Gross-Neveu model, we demonstrate the delicate interplay between kinetic mass, vertex mass and physical mass, which leads to the crucial divergence in the helicity amplitude with the vertex mass factored out. This is necessary to counterbalance the vanishing of the vertex mass, and we explicitly demonstrate that the physical helicity flip amplitude stays finite in the chiral limit.

The calculation was done starting from the canonical LF-Hamiltonian plus a kinetic mass counter-term for the fermions. Even though most of the analysis used the language of diagrams, it should be emphasized that we derived non-perturbative relations between Green's functions. The results thus obtained are therefore equivalent to results that one could also obtain by nonperturbatively solving eigenvalue equations resulting in an infinite number of coupled Fock space equations.

Upon analyzing the physical helicity flip amplitude, one finds that a large amplitude in the chiral limit emerges only after an infinite number of Fock space components have been included. One can draw a number of lessons from this result. First, it seems that a calculation based on a canonical Hamiltonian (plus m_{kin}^2 counter-term) is in principle sufficient to describe a situation where chiral symmetry is dynamically broken. Secondly, from a fundamental point of view, while zero-mode induced corrections seem crucial for kinetic mass generation and thus also for physical mass generation (in the sense of eigenvalue of the invariant mass operator), they are not important for dynamical vertex mass generation (DVMG), i.e. for large physical helicity flip amplitudes and large hyperfine splittings). Instead DVMG comes from high Fock components and thus also the small x region. From the practitioner's point of view our results imply that a calculation based on a canonical Hamiltonian (plus m_{kin}^2 counter-term) must include a very large number of Fock components in the small fermion mass limit in order to generate the physics of dynamical chiral symmetry breaking. Since a sufficiently large number of Fock components may be very difficult to handle adequately in numerical calculations (both using DLCQ or basis functions methods), it may thus be advantageous

to improve the canonical (plus Δm_{kin}^2) Hamiltonian by adding non-canonical terms. In principle, these terms can be obtained by integrating out (or parameterizing) higher Fock components self-consistently.

Given the abovementioned caveats, what can we learn from these results about dynamical chiral symmetry breaking in LFQCD? Of course, this part is only speculation, but there are some very suggestive conjectures that one can make concerning this issue: Several models and approximations to LFQCD, such as dimensionally reduced models [15] or the transverse lattice [16], give rise to effectively 1+1 dimensional theories¹⁵. These models or approximations contain both interactions which resemble interactions in QCD_{1+1} as well as couplings to the transverse gauge degrees of freedom that very much resemble the couplings of the model studied in this paper. As has been pointed out in Ref. [15], the end-point behavior of wave functions for higher Fock components is dominated by the couplings of the fermions to the transverse gauge degrees of freedom and *not* by the longitudinal gauge interaction. Since the non-perturbative enhancement of helicity flip enhancement described in this paper originated in the small k^+ and high Fock component region, one would thus expect that the same or a similar mechanism also works in collinear QCD models as well as on the transverse lattice. If this is indeed the case then it is also clear that numerical techniques based on a Fock space expansion (both DLCQ as well as basis function methods) are doomed to fail in the chiral limit, unless effective interactions are added which mimic the effects from the small k^+ and high Fock component region, which typically has to be omitted for practical reasons. The most simple operator that one might think of based on the results of this paper is a "running vertex mass". Integrating out small k^+ and high Fock components should lead to effective quarks with the following properties: at low momentum transfers and with initial and final states not too far off shell, the quarks in collinear QCD or \perp lattice approaches should acquire a large (constituent mass scale!) effective vertex mass. However, because of asymptotic freedom, one should recover the current quarks when the states are highly off shell. Such features can be incorporated into an effective LF Hamiltonian with a "running" vertex mass. A detailed discussion of this running, which will depend on the precise nature of the model and of the cutoff employed, would go beyond the intended scope of this paper.

¹⁵It should be emphasized that the transverse lattice is still a 3+1 dimensional formulation of QCD. However, since the transverse directions are discretized in this approach, it can formally be regarded as a large number of coupled 1+1 dimensional theories!

ACKNOWLEDGMENTS

I would like to thank the participants of the “International Workshop on Light-Cone QCD and Nonperturbative Hadronic Physics” in Lutsen, MN (August 97) for many inspiring discussions. I would also like to thank Bob Klindworth for reading and criticizing the manuscript. This work was supported by the D.O.E. (grant no. DE-FG03-96ER40965) and in part by TJ-NAF.

- [1] K.G. Wilson et al., Phys. Rev. D **49**, 6720 (1994).
- [2] S.J. Brodsky, H.-C. Pauli and S.S. Pinsky, *Submitted to Phys. Rept.*; S.J. Brodsky et al., Part. World **3**, 109 (1993).
- [3] M. Burkardt, Advances Nucl. Phys. **23**, 1 (1996).
- [4] X. Ji, Phys. Rev. Lett. **78**, 610 (1997); A.V. Radyushkin, Phys. Rev. D **56**, 5524 (1997).
- [5] R.J. Perry, lectures given at NATO Advanced Study Institute on Confinement, Duality and Nonperturbative Aspects of QCD, Cambridge, England, 23 Jun - 4 Jul 1997. e-Print Archive: hep-th/9710175.
- [6] M. Burkardt and H. El-Khozondar, Phys. Rev. D **55**, 6514 (1997).
- [7] M. Burkardt, Phys. Rev. D **47**, 4682 (1993); E. Prokhorov et al., Phys. Rev. D **51**, 2933 (1995); J.P. Vary et al., Phys. Rev. D **53**, 7231 (1996).
- [8] M. Burkardt, Phys. Rev. D **54**, 2913 (1996).
- [9] M. Burkardt and A. Langnau, Phys. Rev. D **44**, 1187; **44**, 3857 (1991).
- [10] K.G. Wilson and M. Brisudova, Proc. 4th Int. Workshop on Light-Front Quantization and Non-Perturbative Dynamics, Ed. S.D. Glazek, (World Scientific, Singapore, 1994).
- [11] S.J. Brodsky, J.R. Hiller and G. McCartor, *submitted to Phys. Rev. D*. e-Print Archive: hep-th/9802120.
- [12] A. Casher and L. Susskind, Phys. Rev. D **9**, 436 (1974).
- [13] L.S. Kisslinger and T. Meissner, Phys. Rev. D **57**, 1528 (1998).
- [14] A.P. Szczepaniak and E.S. Swanson, Phys. Rev. D **55**, 1578; 3987 (1997).
- [15] F. Antonuccio and S. Dalley, Phys. Lett. B **376**, 154 (1996).
- [16] W. A. Bardeen, R. B. Pearson and E. Rabinovici, Phys. Rev. D **21**, 1037 (1980).